Gated negative-effective-mass ballistic terahertz generators

A. N. Korshak, Z. S. Gribnikov,[a] N. Z. Vagidov, and V. V. Mitin
Department of Electrical and Computer Engineering, Wayne State University, Detroit, Michigan 48202

(Received 17 June 1999; accepted for publication 13 August 1999)

We consider gate control of terahertz generation in planar ballistic diodes with a negative-effective-mass section in a dispersion relation of current carriers in a current-conducting channel. Such a generation in ballistic p^+pp^+ or n^+nn^+ diodes occurs as a result of plasma instability development and self-organization of a regular oscillation regime. Conditions of existence and oscillation frequencies are calculated. The gate can also serve as an oscillation-collecting electrode. We consider double-gate designs, side by side with conventional single-gate designs. The double-gate devices allow us to separate circuits for direct and high-frequency currents. [S0003-6951(99)00141-2]

Two diverse designs of the negative-effective-mass (NEM) ballistic terahertz generators have recently been suggested: the vertical design[1] and the horizontal design.[2,3] The former is based on ''natural'' band-structure NEM mechanisms,[4,5] or on a NEM mechanism in valence bands of uniaxially compressed p-type diamond-like and zinc-blende-like semiconductors.[1,6] This design anticipates a layer by layer growth of multilayer p^+pp^+ or n^+nn^+ structures with strictly given parameters. The horizontal design is based on NEM mechanisms, which are inherent in some two-dimensional (2D) electron[2] and hole[3] gases. These mechanisms are much more flexible and can be electrically tuned. But formation of p^+pp^+ or n^+nn^+ diode structures using these NEM mechanisms (in very short p- or n-planar bases and with precisely given parameters of p^+ or n^+ regions) is much more awkward.

In this letter we consider only horizontally designed p^+pp^+ diodes with p-type quantum well (p-QW) bases. (These diodes seen as NEM ballistic terahertz generators are theoretically described in great detail in Ref. 3.) To avoid extremely short bases we introduce new elements in diode design: gates. These gates have to control a channel charge in the current-conducting p-QW channels under the gates. Here we suggest two variants of diodes with such gated bases: a single-gate diode [Fig. 1(a)] and a double-gate diode [Fig. 1(b)]. The initial concept of the single-gate diode is forming a comparatively depleted channel segment under the gate in the background of the heavily doped base. This depleted segment has to play a role of an effective base (EB). The ungated left- and right-hand side segments [in Fig. 1(a)] of the base (which are undepleted as a result) play the roles of effective anode and effective cathode, respectively. The gate length determines the length of the EB, and positive gate potential controls hole depletion in the EB.

The initial concept of the double-gate diode is forming a comparatively depleted channel segment in the central section between the gates. The gated left- and right-hand side segments of the base [in Fig. 1(b)] are enhanced by holes caused by negative gate potentials. Therefore the central ungated segment of the base channel is an EB, and the gated left- and right-hand side segments are an effective anode and cathode, respectively. Both above-presented prescriptions allow us to control hole concentrations in the effective anode, base, and cathode accurately and in very wide ranges. A gate length, l_g, for the single-gate design, as well as a distance between the gates, l_s, for the double-gate design can now each be made very short. This means that EBs can be very short. All these reasons are tested by the calculations described below.

We consider a one-dimensional (1D) transport of ballistic holes with a dispersion relation $\epsilon(k)$ shown in the inset in Fig. 1. Here $k=|\mathbf{k}|$; $\mathbf{k}=(k_x,k_y)$ is a wave vector of quantized holes in a square 8 nm GaAs p-QW with AlAs barriers (see details in Ref. 3). This p-QW serves as a current-conducting channel that connects a plane source (anode) with a plane drain (cathode). We assume that holes from the source and the drain enter this channel being Fermi–Dirac distributed with identical Fermi energies μ (~10–20 meV). The entered holes move in electric fields, which are formed by ionized acceptors, by self-consistent spatial charge of all other holes, and by given potentials of the drain (U_d), the

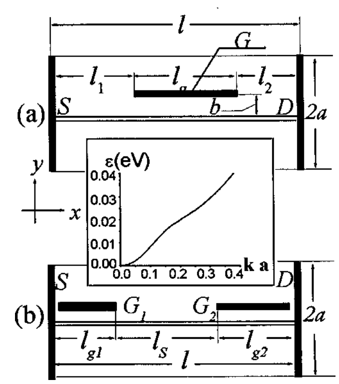

FIG. 1. Sketches of single-gate (a) and double-gate (b) ballistic generator structures. The dispersion relation of quantized holes in square 8 nm GaAs/AlAs p-QW used for calculations is shown in the inset (**ka** is a product of a wave vector and a lattice constant).

[a]Electronic mail: zinovi@besm6.eng.wayne.edu

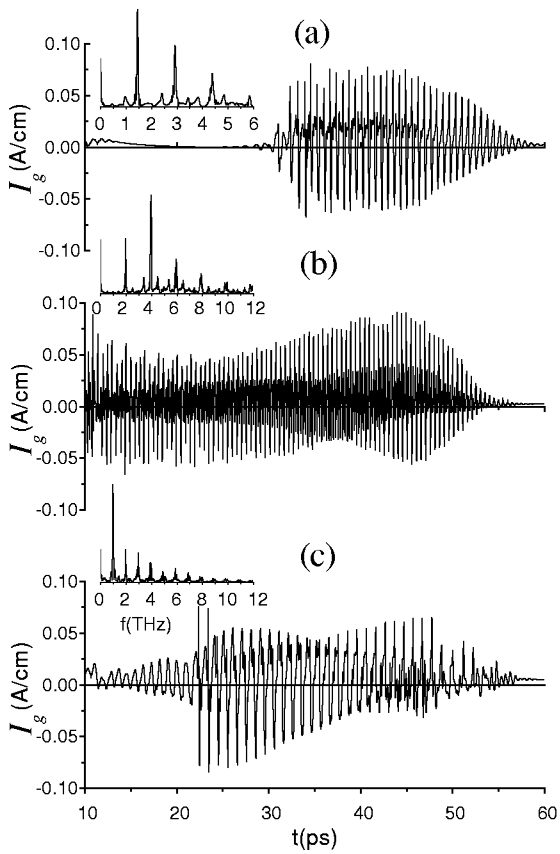

FIG. 2. Gate currents, I_g, of a single-gate device vs time, t, for cases A (a), B (b), and C (c). $U_d = -40$ mV, U_g changes adiabatically slow: $U_g = -50\ \text{mV} + U_g' \times t$, where $U_g' = 1$ mV/ps. Parameters used for calculations: $l = 0.2\ \mu$m, $l_g = 0.033\ \mu$m, $b = 0.016\ \mu$m, $N_a = 1 \times 10^{11}\ \text{cm}^{-2}$, dielectric constant $\kappa_d = 10.9$, temperature $T = 4.2$ K, $\mu = 10$ meV. Case A: $l_1 = l_2 = 0.083\ \mu$m; case B: $l_1 = 0.061\ \mu$m, $l_2 = 0.105\ \mu$m; case C: $l_1 = 0.105\ \mu$m, $l_2 = 0.061\ \mu$m. The results of Fourier analysis of the gate currents are shown in the insets.

gates (U_g, $U_{g1,2}$), and the source ($U_s = 0$). We place the ionized acceptors with concentrations $N_a = 8 \times 10^{10} - 2 \times 10^{11}\ \text{cm}^{-2}$ directly into the p-QW for simplification. However, we are keeping in mind a modulation-doped structure with acceptor sheets in the barriers. We use conditions of periodicity (with spatial period $2a = 0.16\ \mu$m along the y axis; see Fig. 1) as boundary conditions in the vertical direction. The parallel diodes can be considered almost independent for this value of $2a$ (see Ref. 3).

A 1D ballistic nonstationary kinetic equation for holes in the current-conducting channel is solved self-consistently with a 2D Poisson equation in all the space between the drain and the source planes. The general scheme of numerical solution of a 1D kinetic equation, solved together with a 2D Poisson equation, is described thoroughly in Ref. 2. We consider diodes with base lengths $l = 0.2$ and 0.5 μm and with gate lengths l_g, $l_{g1,2}$ down to 0.033 μm. [Let us note that modern high-speed field effect transistors (FETs) with similar base and gate sizes are now actually manufactured.][7] Terahertz generation in wide ranges of drain and gate voltages is observed as a result of completed calculations in both considered variants of structures.

The considered single-gate diodes are of $l = 0.2\ \mu$m and $l_g = 0.033$ and 0.08 μm. (Other structure parameters are indicated in the caption to Fig. 2.) The results for these two gate lengths l_g are almost identical. A drain current I_d changes with changes in U_g slowly for negative and near to 0 gate potentials. Therefore, dependence $I_d = I_d(U_d)$ is qualitatively the same as for ungated diodes.[3] Positive gate potentials U_g, which exceed $\sim$10 mV, depress the drain current linearly with increasing U_g down to full locking. As a rule, terahertz current oscillations exist in a wide range of negative drain and gate potentials (for example, for $U_d < -20$ and 5 mV$> U_g > U_d$).

Spatial distributions of electric potential and hole concentration in the channel show that a base segment between the source and the gate does not play a noticeable role in the oscillation process. Main events take place in the space between the gate and the drain, which also includes a drain side of the gated segment. In practice, a greater part of the drain-source voltage U_d drops across this region. Holes, which are moving from the source to the drain, also reach the NEM section of the dispersion relation in this space. Therefore, a traveling dipole domain of accumulation–depletion is formed near the gate edge and moves to the drain. It seems that the ballistic diode as a whole is contracted up to the right-hand side part of the base and the effective cathode is shifted to the gated segment. Such an image reminds us of the analogous domain image for a gate-controlled Gunn generator, where dipole domains also travel only in a gate-drain space (see Ref. 8 and references therein). Almost all of the high-frequency drain current is a displacement current of the gate. We have no substantial oscillations of the source current.

Side by side with the central gate position in the base (case A), we consider two added cases with 0.022 μm shifted to the source and to the drain gates (cases B and C, respectively). Three portraits of gate current oscillations for cases A, B, and C are presented in Fig. 2. (All other design parameters and voltages are identical for all three cases.) We can see that the comparatively small shift of the gate from the central position perturbs the oscillation picture and has a very noticeable influence on the oscillation frequency. Beyond all expectations in the considered situation the frequency increases for case B and decreases for case C (see Fourier analysis results in the insets in Fig. 2). More detailed consideration shows that we have obtained a two-dipole-domain regime in the extended gate-drain segment for case B. This regime is much faster than the simple single-domain regime. For case C we have some added oscillation activity in the extended source-gate segment (which is absent in cases A and B). This activity decreases the bound-oscillation frequency in the combined plasma cavity. We pay attention to very high (at the considered sizes) frequencies of the first and the second harmonics ($\sim$2 and 4 THz) for case B.

Most of the considered double-gate diodes have base length $l = 0.5\ \mu$m and gate lengths $l_{g1} = l_{g2} = 0.085\ \mu$m. The gates G_1 and G_2 are brought near the source and the drain, respectively, but all of the electrodes are isolated from each other and have independent potentials $U_s = 0$, U_{g1}, U_{g2}, and U_d. The length of the ungated spacer between the gates is of $l_s = 0.33\ \mu$m. We keep (for our numerical measurements) a regime with a given potential of gate 1 relatively to the source, U_{g1}, and with the same potential of gate 2 relatively to the drain, that is $U_{g2} = U_d + U_{g1}$. For the working regimes

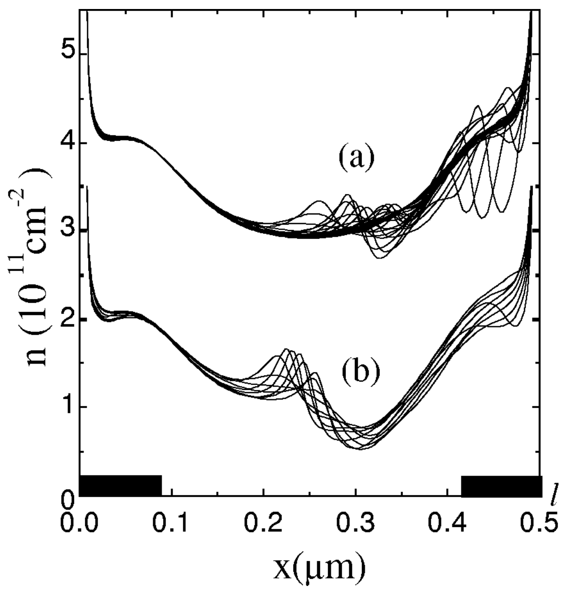

FIG. 3. Snapshots of concentration distributions, $n(x)$, in the base of the double-gate device for two different stages of oscillation process: (a) small drain voltages (20–40 mV); (b) large drain voltages (50–65 mV). Sample parameters: $l=0.5\,\mu$m, $l_{g1}=l_{g2}=0.085\,\mu$m, $b=0.064\,\mu$m, $N_a=8\times10^{10}\,\mathrm{cm}^{-2}$, $\mu=20$ meV; all other parameters are the same as in Fig. 2. Distributions (a) are $2\times10^{11}\,\mathrm{cm}^{-2}$ shifted upward.

all these potentials are negative. A drain current rises fast with the increase in $|U_d|$ up to the NEM section in the dispersion relation but it is not saturated completely after reaching this section, due to such an increase in $|U_{g2}|$ as in $|U_d|$.

Concentration distributions in the base of one of the double-gate diodes are presented in Fig. 3. The enhancing gates provide the distribution with a depleted region between two enhanced regions. We obtain a p^+pp^+ structure with smooth boundaries of the p region. The oscillations appear just in this p region and have a structure that reminds us of the oscillation structure in p^+pp^+ diodes with sharp edges of the p base.[3] A region where oscillations initiate shifts with increasing $|U_d|$ to the source. The concentration oscillations are localized in the middle of the base in the final stage of the oscillation process for large values of $|U_d|$. Oscillation activity depends on gate lengths $l_{g1,2}$. It is greater for shorter gates and can be suppressed if gates are too long. The oscillation frequency for all the calculated double-gate structures is around 0.7 THz (that is approximately the same as for 0.3-μm-base p^+pp^+ diodes but much higher than for 0.5-μm-base diodes).

In conclusion, we have found that the controlling gates that are applied to design of ballistic NEM diodes improve generator functional opportunities. The gates allow us to reach higher oscillation frequencies in comparison with ungated diodes for the same base lengths. This is a result of redistribution of electric fields in the base as well as effective shortening of active region lengths with plasma instability. The gates collect high-frequency currents and separate paths of these currents from the emitting source at the single-gate design (and from the entire direct current path at the double-gate design). Gate potentials allow us to control frequency and amplitude of high-frequency current, as well as to turn this current on and off. We have found that single-gate NEM devices are successful in the enhancement mode and the shallow depletion mode, and they do not generate in the deep depletion mode. Shallow depletion provides an effective control of oscillation amplitude. The double-gate NEM devices confirms their initial concept well.

To be implemented the suggested devices require high level technology but this level does not exceed present technological level of the highest-speed MODFETs (excluding the necessity of lower working temperatures: $\leqslant$10–20 K and lighter modulation doping: $\sim10^{11}\,\mathrm{cm}^{-2}$).

The authors thank O. Melnikova for helpful discussions. This work was supported by the NSF Grant and JPL DFDR Grant.

[1] N. Z. Vagidov, Z. S. Gribnikov, and A. N. Korshak, Semiconductors **31**, 150 (1997).

[2] Z. S. Gribnikov, A. N. Korshak, and N. Z. Vagidov, J. Appl. Phys. **80**, 5799 (1996).

[3] Z. S. Gribnikov, A. N. Korshak, and V. V. Mitin, Int. J. Infrared Millim. Waves **20**, 213 (1999).

[4] M. L. Cohen and J. R. Chelikovsky, *Electronic Structure and Optic Properties of Semiconductors* (Springer, Berlin, 1988).

[5] Yu. M. Sirenko, J. B. Leon, B. C. Lee, K. W. Kim, M. A. Littlejohn, M. A. Stroscio, and G. J. Iafrate, Phys. Rev. B **55**, 4360 (1997).

[6] G. Bir and G. Pikus, *Symmetry and Strain Induced Effects in Semiconductors* (Wiley, New York, 1974).

[7] D. Xu, T. Suemitsu, J. Osaka, Y. Umeda, Y. Yamane, Y. Ishii, T. Ishii, and T. Tamamura, IEEE Electron Device Lett. **20**, 206 (1999).

[8] Z. S. Gribnikov and V. B. Zheleznyak, Sov. Phys. Semicond. **25**, 9 (1991).